Journal of Molecular Structure 1137 (2017) 403–411

Contents lists available at ScienceDirect

Journal of Molecular Structure

journal homepage: http://www.elsevier.com/locate/molstruc

Physical and optical properties of DCJTB dye for OLED display applications: Experimental and theoretical investigation

Mustafa Kurban [a, b, *], Bayram Gündüz [c]

[a] Department of Electronics and Automation, Ahi Evran University, 40100 Kırşehir, Turkey
[b] Department of Physics, Middle East Technical University, 06800 Ankara, Turkey
[c] Department of Science Education, Faculty of Education, Muş Alparslan University, 49250 Muş, Turkey

ARTICLE INFO

Article history:
Received 9 January 2017
Received in revised form
3 February 2017
Accepted 4 February 2017
Available online 20 February 2017

Keywords:
Optical techniques
Structure analysis
Optical properties
Electronic properties
Density-functional theory

ABSTRACT

In this study, 4-(dicyanomethylene)-2-*tert*-butyl-6-(1,1,7,7-tetramethyljulolidin-4-yl-vinyl)-4*H*-pyran (DCJTB) was achieved using the experimental and theoretical studies. The electronic, optical and spectroscopic properties of DCJTB molecule were first investigated by performing experimental both solution and thin film techniques and then theoretical calculations. Theoretical results showed that one intense electronic transition is 505.26 nm a quite reasonable and agreement with the measured experimental data 505.00 and 503 nm with solution technique and film technique, respectively. Experimental and simple models were also taken into consideration to calculate the optical refractive index (n) of DCJTB molecule. The structural and electronic properties were next calculated using density functional theory (DFT) with B3LYP/6-311G (d, p) basis set. UV, FT-IR spectra characteristics and the electronic properties, such as frontier orbitals, and band gap energy (E_g) of DCJTB were also recorded time-dependent (TD) DFT approach. The theoretical E_g value were found to be 2.269 eV which is consistent with experimental results obtained from solution technique for THF solvent (2.155 eV) and literature (2.16 eV). The results herein obtained reveal that solution is simple, cost-efficient and safe for optoelectronic applications when compared with film technique.

1. Introduction

In recent years, organic dyes have attracted enormous attention due to their easy molecular tailoring, very strong light-harvesting ability, rich photo physical properties and high extinction coefficients [1]. Among the organic dyes, 4-(dicyanomethylene)-2-*tert*-butyl-6-(1,1,7,7-tetramethyljulolidin-4-yl-vinyl)-4*H*-pyran (DCJTB) has been subject of intense research for variety of applications that are used as red dopant, quest and host material [2], green emission source [3] and an elegant red fluorescent dye [4] due to its high luminance efficiency, better colour purity, and resistance to concentration quenching for organic light-emitting diodes (OLEDs) display applications. Recently, the photovoltaic performance of dye-sensitized solar cells has been improved by using DCJTB interface modification with combining effects of retarding the charge recombination and Förster resonance energy transfer [5]. Researchers also show that doping DCJTB into the co-host matrix emitting system of rubrene/Alq_3 helps solve the problem of luminescence quenching at high drive voltage [6]. In addition, ultrathin layer of various fluorescent DCJTB dyes has been inserted between acceptor and donor heterojunction to form additional exciton separation interfaces between the dye and acceptor in small molecule organic solar cells [7–9]. The utilization of fluorescent dye particularly DCJTB as the surface modifier of ZnO nanorods in hybrid solar cell application has also been found to be resulted in higher exciton dissociation efficiency which leads increased current density and circuit voltage [10]. It is also indicated that the red dye DCJTB encapsulated in silica SBA-15 has showed lower stimulated-emission threshold, larger net gain, and lower loss coefficient [11].

In the present work, we report optoelectronic properties of DCJTB using solution and film techniques. Different relations were also performed to calculate the optical refractive index (n) values of DCJTB molecule. These properties were controlled with different solvents and film thicknesses. The structural, electronic and spectroscopic properties of DCJTB molecule have been investigated by performing density functional theory (DFT) calculations. The

* Corresponding author. Department of Electronics and Automation, Ahi Evran University, 40100 Kırşehir, Turkey.
E-mail address: mkurbanphys@gmail.com (M. Kurban).

http://dx.doi.org/10.1016/j.molstruc.2017.02.064
0022-2860/

theoretically predicted the ultraviolet–visible (UV–Vis), Fourier transform infrared (FT-IR) spectra characteristics, the highest occupied molecular orbital (HOMO), the lowest unoccupied molecular orbital (LUMO) and the frontier molecular orbital energy gap (HOMO–LUMO difference in energy gap, E_g) of DCJTB molecule using time dependent (TD)-DFT based on optimized structure with different solvent environments have been compared with the experimentally measured and the results have been discussed in detail.

2. Experimental details

2.1. Preparation of the solutions and thin films

Solution and film techniques have been used in the preparation of solutions and thin films of DCJTB organic semiconductor dye to investigate spectroscopic, electronic and optical properties. The DCJTB organic dye molecule is provided from Sigma-Aldrich Chemical Company (USA) with a stated purity of 99% (HPLC). The solutions of the DCJTB organic dye for 21.72 μM have been prepared for different solvents such as acetone, chloroform, dichloromethane (DCM), n-hexane and tetrahydrofuran (THF), and then the weighed DCJTB dyes were dissolved homogeneously in 8 mL volume of the related solvents. On the other hand, several steps were involved in the preparation of the thin films of the DCJTB with different film thicknesses which were randomly obtained. The steps are explained in details as below. Before deposition, we first cut the glass slides, whose dimensions are 25 mm × 75 mm with a diamond cutter and the glass slides thoroughly cleaned with deionized water (DIW) and hydrochloric acid (HCl-37%) to remove glass grains and oxide impurities. Then, the glass slides were extensively rinsed with DIW to remove the residual HCl and cleaned with ethanol to remove organic impurities. Finally, these slides were dried with pressurized nitrogen. Therefore, DCJTB thin films were deposited on cleaned and dried glass slides by dropping and shaking coating method. After coating, solvent evaporation was completed at room temperature for 30 min in order to dry DCJTB thin films. The film thicknesses of the DCJTB films were determined with a thickness gauge/micrometer (ASIMETO model) and were found to be 12, 22 and 28 μm.

2.2. The UV and FT-IR measurements

The UV and FT-IR spectra measurements were also recorded using the solution and film techniques. The Hellma QS-100 cylindrical bathtub, which have 3.5 mL volume and 10 mm optical path length, was used for all the solutions of the DCJTB organic dyes solved in acetone, chloroform, DCM, n-hexane and THF solvents. The UV measurements of the solutions of the DCJTB organic dye with different thin film thicknesses (12, 22 and 28 μm) were recorded with a Shimadzu model UV-1800 Spectrophotometer in the wavelength of 1100–190 nm at room temperature. FT-IR measurements were recorded with a KBr quartz containing chloroform, DCM and THF solvents on a Perkin-Elmer Precisely Spectrum One Spectrometer at room temperature between 450 and 4000 cm^{-1}.

2.3. Theoretical considerations

The mass extinction coefficient ($\alpha_{mass}\,(Lg^{-1}cm^{-1})$) is an important parameter for optoelectronic applications and is given by Refs. [12,13],

$$\alpha_{mass} = \frac{\varepsilon}{M_A} \tag{1}$$

where $\varepsilon\,(Lmol^{-1}cm^{-1})$ is the molar extinction coefficient and M_A is the molecular weight (g/mol). The optical band gap $E_g\,(eV)$, dependent absorption coefficient ($\alpha\,(cm^{-1})$) and photon energy ($h\upsilon\,(eV)$) can be expressed by Ref. [14],

$$\alpha(h\upsilon) = B\left(h\upsilon - E_g\right)^{1/2} \tag{2}$$

where B is a constant.

The refractive index, n, can be calculated using the following equation [15,16]:

$$n = \left\{\left[\frac{4R}{(R-1)^2} - k^2\right]^{1/2} - \frac{R+1}{R-1}\right\} \tag{3}$$

where k is the wavelength and R is the reflectivity.

The relation between E_g and n of semiconductors can be given with many relations such as Moss, Ravindra, Hervé-Vandamme, and Kumar-Singh [17].

Moss relation connecting E_g to n of semiconductors is given by

$$n^4 = \frac{95\ eV}{E_g} \tag{4}$$

Ravindra relation [18] which represents a linear relation governing the variation of n with E_g is defined as:

$$n = 4.084 - 0.62E_g \tag{5}$$

In the Hervé and Vandamme relationship,

$$n^2 = 1 + \left(\frac{A}{E_g + B}\right)^2 \tag{6}$$

where A is the ionization energy of the hydrogen atom in its ground state and B is a constant assumed to be the difference between E_g and UV resonance energy. A and B are 13.6 and 3.47 eV, respectively [19].

The correlation between n and E_g for Kumar and Singh relation is given by

$$n = \frac{3.3668}{(E_g)^{0.32234}} \tag{7}$$

3. Computational details

The structural, electronic and spectroscopic properties of DCJTB dye have been investigated using DFT [20] at the B3LYP level [21–23]. The 6-311G (d, p) basis set has been used in the calculations. The calculations have been performed using the GAUSSIAN09 program package [24]. Various spin multiplicities were investigated and it has been found that DCJTB have spin singlet as the most stable (minimum total energy). The structure is taken as the local minima on potential energy surface having positive vibration frequencies. After geometric optimization, TD-DFT method used to get maximum wavelengths and compared with the experimental UV, FT-IR absorption, HOMO, LUMO and E_g of DCJTB. . Theoretical results identified that the structure with minimum total energy of DCJTB molecule is the C_1 form. Optimized ground state structure and process of geometry optimization of DCJTB with atom numbering calculated by B3LYP/6-311-G (d,p) is shown in Figs. 1 and 2, respectively.

4. Results and discussion

4.1. Experimental and theoretical infrared spectra results

The FT-IR spectra of the DCJTB dye were taken for acetone, chloroform and DCM solvents in the range 450–4000 cm^{-1} with a KBr quartz and shown in Fig. 3 (a). As seen in Fig. 3 (a), for chloroform and DCM solvents, there is a very strong and sharp peak at 2360 cm^{-1}, which can be assigned asymmetrical stretch O=C=O, that is, this strong peak shows the presence of atmospheric carbon dioxide, CO_2. However, DCJTB dye for acetone solvent exhibits a medium peak at 2359 cm^{-1}, which due to the H bonded O–H stretching carboxylic acid [25], the C≡N stretch nitriles, C=C alkyne stretching [26], asymmetric stretching mode of CO_2 [27] and the –OH stretching vibrations of acid dimers [28]. The DCJTB dye exhibits a medium and sharp peak for chloroform and DCM at 668 cm^{-1}, which can be attributed to metal–oxygen (M–O) stretching vibrations [29] and C–H out of plane bending [30]. The DCJTB indicates a medium and sharp peak for DCM at 1185 cm^{-1}, which can be assigned to C–C band [31] and C–H stretching modes of CH_3 and CH_2 groups. The DCJTB shows medium and sharp peak for DCM at 1642 cm^{-1}, which can be attributed to typical anti-symmetric stretching band, H–O–H bending of water [32] and C=C stretching band. The DCJTB dye indicates a weak and sharp peak for acetone, chloroform and DCM solvents at 2207 cm^{-1}, which can be assigned to –CN [33], –C=C– stretching vibrations and stretching vibration of the cyano group [34]. The DCJTB dye has a pair of weak peaks for DCM at 2851 and 2922 cm^{-1}, which corresponds to the symmetrical and asymmetrical stretching vibrations of methylene group (CH_2) in an aliphatic hydrocarbon [35]. Furthermore, the peak at 2851 cm^{-1} can be attributed to C–O bonds [36], aliphatic –CH, C–H stretching of sp^3 carbon, CH_2 symmetric stretching [37].

From TD-DFT calculations, the positive vibrational spectra, that is no any kind of imaginary frequency, are found that the optimized geometry of the DCJTB compound is located at stationary point on the potential energy surface. Theoretically simulated FT-IR spectra for DCJTB are shown in Fig. 3 (b). From Fig. 3 (a) and (b), the theoretically simulated spectra are found to be more regular than measured ones due to some vibrations presenting in condensed phase. The theoretical and experimental scaled wavenumber for

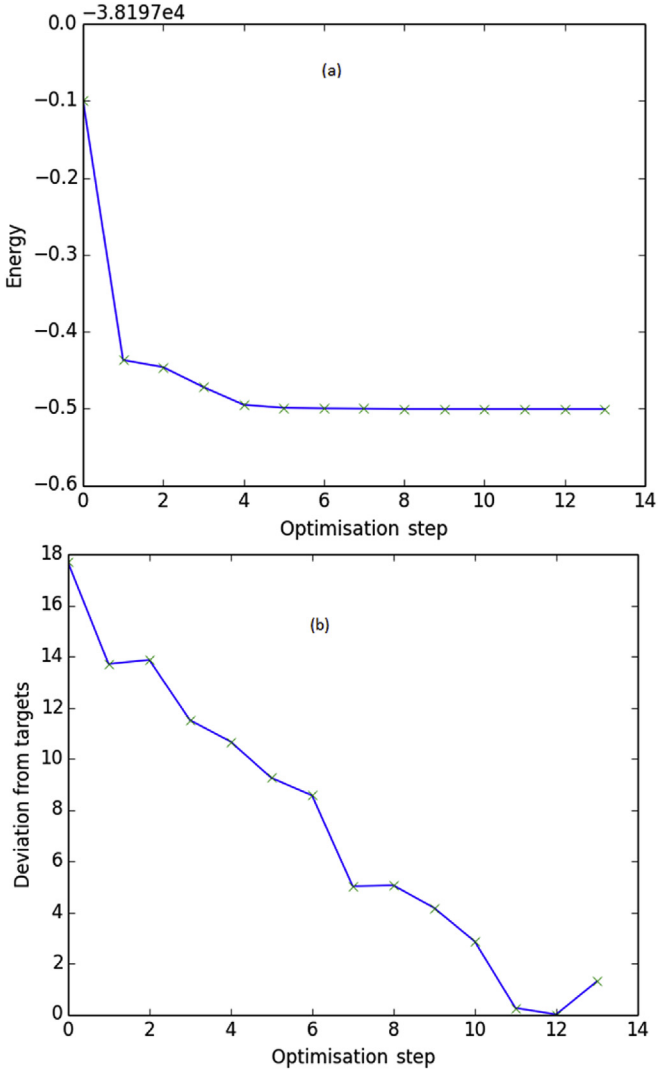

Fig. 2. Process of geometry optimization of DCJTB depending on (a) energy (b) derivation from targets.

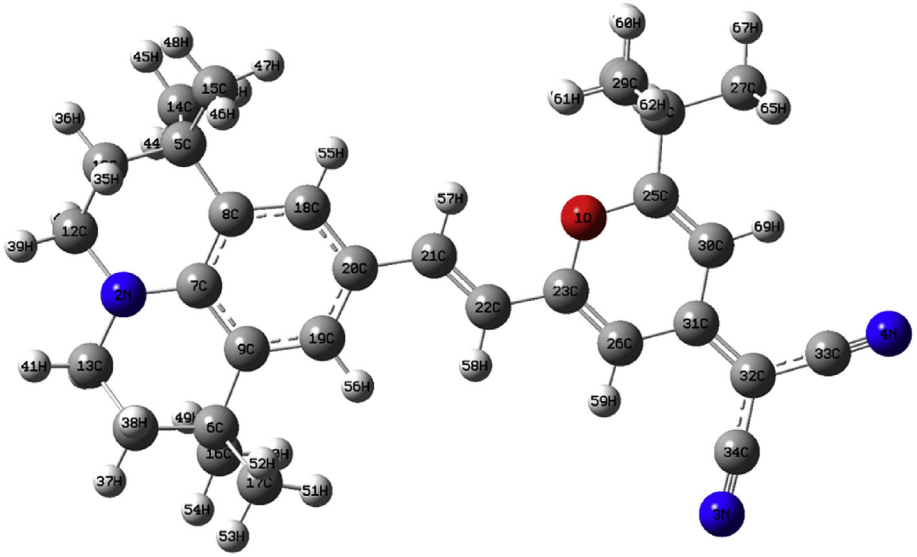

Fig. 1. Optimized ground state geometry of DCJTB molecule with atom numbering calculated by B3LYP/6-311-G(d,p).

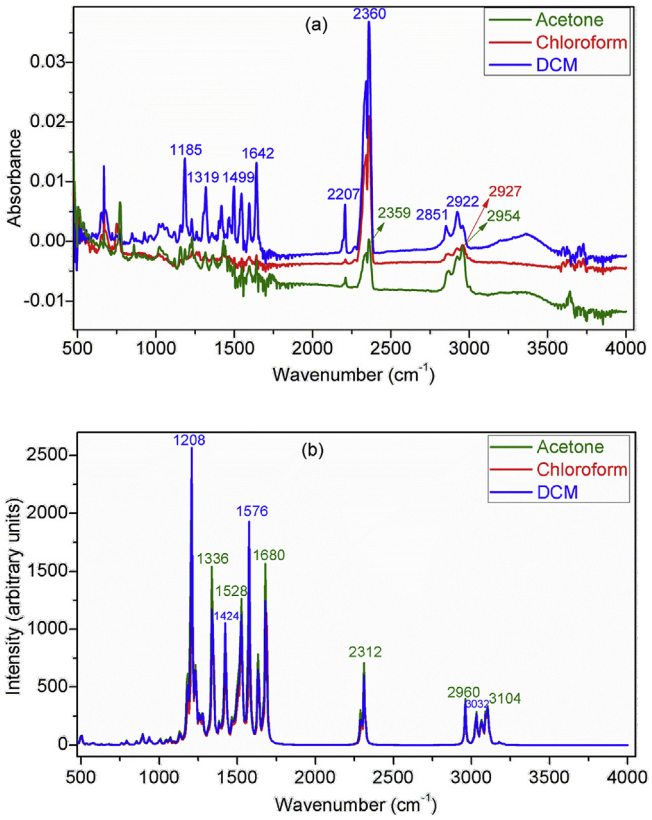

Fig. 3. **(a)** The experimental and **(b)** simulated infrared spectra of DCJTB dye for different solvents.

acetone solvent is found to be well matched as 2960 and 2954 cm^{-1}, respectively.

4.2. Experimental and theoretical absorption characteristics

Fig. 4 shows the absorbance curves of the DCJTB films for different thickness. The absorbance of DCJTB film decreases with decreasing film thicknesses and the wavelength which is observed at maximum absorbance changes with film thicknesses. The maximum peak position or wavelength values for 12, 22 and 28 μm were found to be 513, 503 and 500 nm, respectively. The position of peaks and corresponding values are displayed in Fig. 4. These results indicate that the film thickness has significant effect on optoelectronic properties for DCJTB film.

The absorbance curves of the DCJTB dye for acetone, chloroform, DCM, n-hexane and THF solvents for 21.72 μM are shown in Fig. 5(a–e), respectively. As shown in Fig. 5(a–e), the absorbance spectra of DCJTB dye have trenches and peaks in the near ultraviolet (NUV) and visible (V) regions. The absorbance spectra for acetone, chloroform, DCM, n-hexane and THF solvents exhibit maximum peaks at 505, 509, 507, 472 and 502 nm of the V region, respectively. We have also observed that the spectra remain almost constant after about 620 nm. These results showed that the solvents have effect on the maximum peak position or wavelength of the absorbance spectra of DCJTB. It is interesting to note that n-hexane solvent has maximum peak at 472 nm. TD-DFT/B3LYP/6-311G (d, p) level of theory predicted one intense electronic transition for DCJTB with solvent acetone 505,26 nm which is a quite reasonable and agreement with the measured experimental data 505.00 nm with solution technique and 503.00 nm with film technique as it is shown in Fig. 5 (a). The maximum absorption wavelength in

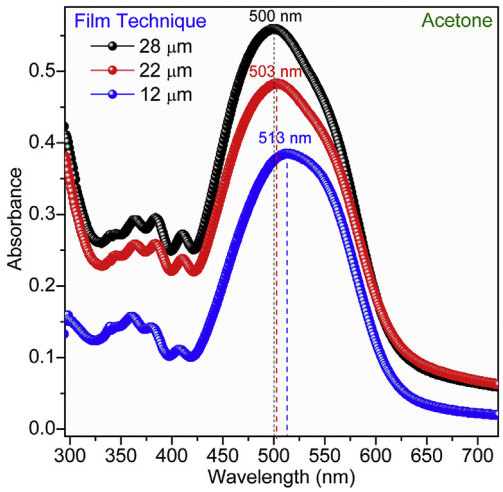

Fig. 4. The absorbance spectra curves vs. wavelength of the DCJTB films for 12, 22 and 28 μm film thicknesses.

acetone corresponds to the electronic transition from HOMO to LUMO with 99% contribution for the calculated absorption spectra.

4.3. Experimental and theoretical energy gap determination

Figs. 6 and 7 demonstrate the variation of $(\alpha h\nu)^2$ versus $E(h\nu)$ for DCJTB solutions and thin films, respectively. The linear region (the best fitting of results) shows that the type of electron transition for DCJTB solutions and thin films is direct allowed transition. E_g is determined by means of extrapolating the linear region of Figs. 6 and 7. Experimentally, several methods have been carried out to determine E_g values for DCJTB solutions and thin films with different solvents and thickness, respectively. We also proposed another method, which is based on the TD-DFT calculations for the determination of E_g. The measured and calculated E_g values are tabulated in Tables 1 and 2. As it is seen, the energy gap of DCJTB dye compound for acetone and THF solvents as the results gives reasonable values than that of the rest solvents. For example, the measured E_g obtained from solution technique for THF solvent and literature is about 2.155 and 2.16 eV, respectively, which is consistent with the theoretical E_g value, 2.269 eV (see Table 1). From the results, one can conclude that acetone solvent with the lowering of E_g can be preferred for optoelectronic applications or devices, which require lower E_g. Moreover, the dispersion of the electronic bands for thicker DCJTB samples increases due to interacting layers and thus reduces E_g as it seen in Table 2. We can also see that E_g decrease with increasing the size of the materials at the nanoscale (see Table 2). This is the most remarkable feature of nano material because we have already observed the same properties in our previous theoretical calculations related to small cluster [38].

The frontier molecular orbital energies were also calculated with TD-DFT//B3LYP/6-331 G(d, p) level. 3D plots of HOMO), LUMO and energy gap, E_g for THF have been given in Fig. 8. Obtained theoretical results for different solvents are given along with the experimental ones from the literature in Table 1. The calculated energy value of HOMO is −5.242, −5.269, −5.252, −5.256 and −5.231 eV in acetone, chloroform, DCM, THF and n-hexane, respectively, which is consistent with the experimental E_g value, −5.26 eV [39,40]. Similarly, LUMO is −2.946, −2.977, −2.977, −2.986 and 2.952 in acetone, chloroform, DCM, THF and n-hexane, respectively. The values is found to be consistent with the measured E_g values, 3.10 and 3.03 eV [39–41]. When taking into consideration experimental techniques

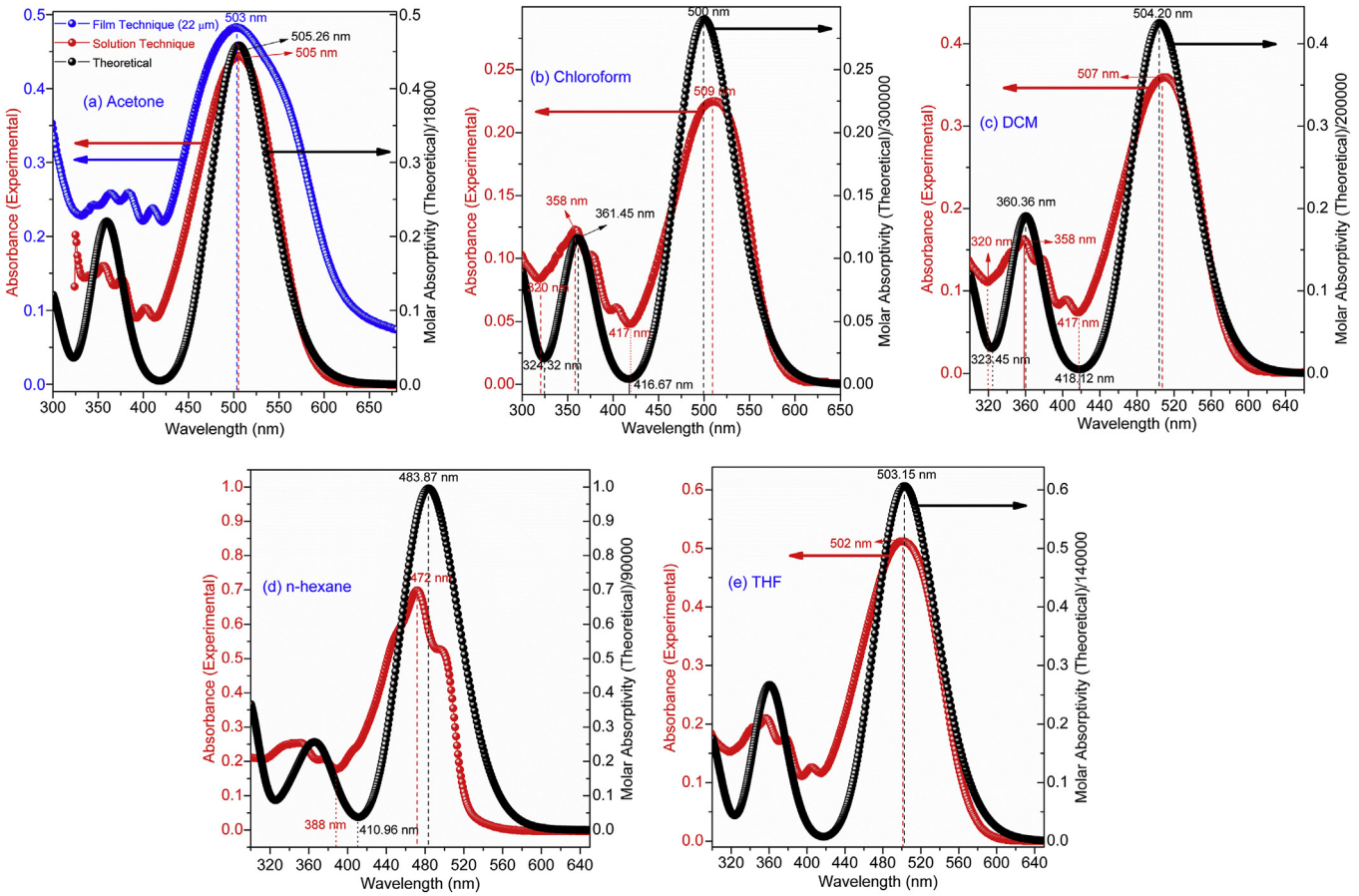

Fig. 5. The experimental UV absorbance spectra and theoretical molar absorptivity plots vs. wavelength (λ) of the DCJTB for **(a)** acetone, **(b)** chloroform, **(c)** DCM, **(d)** n-hexane and **(e)** THF solvents for 21.72 μM (Figure (a) includes solution and film techniques as well as theoretical calculation, the rest of figures include solution technique and theoretical calculation).

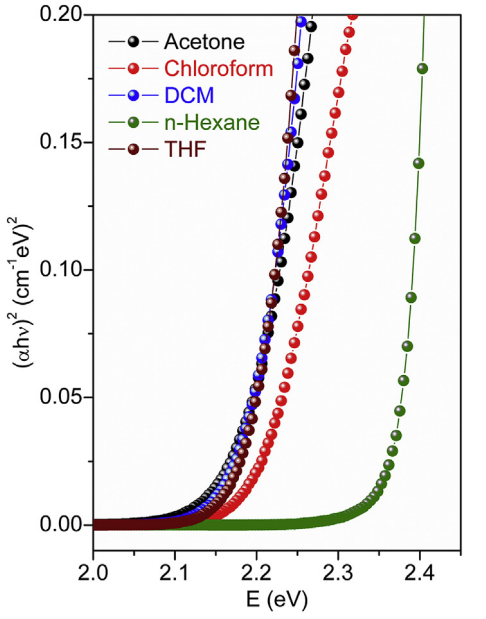

Fig. 6. The $(\alpha h\upsilon)^2$ plot vs. photon energy (E) of the DCJTB solutions for acetone, chloroform, DCM, n-hexane and THF solvents.

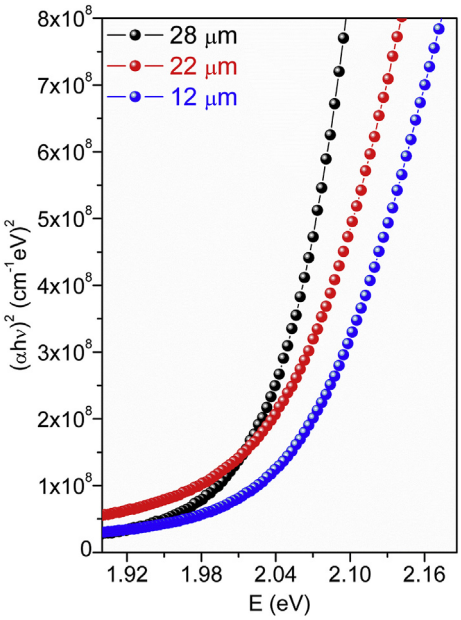

Fig. 7. The $(\alpha h\upsilon)^2$ plot vs. E of the DCJTB films for 12, 22 and 28 μm film thicknesses.

Table 1
The calculated energies and energy gaps (E_g) between HOMO and LUMO orbitals of DCJTB for different solvents. (Acetone (A), Chloroform (C), Dichloromethane (DCM), tetrahydrofuran (THF), n-Hexane (n-H).

Energy level (eV)	Exp.[a,b,c]	TD-DFT/6-311G (d, p)/(Exp.)				
		A	C	DCM	THF	n-H
HOMO	5.26[a,b], 5.10[c]	5.242	5.269	5.252	5.256	5.321
LUMO	3.10[a,b], 3.03[c]	2.946	2.997	2.977	2.986	2.952
E_g	2.16[a,b], 2.07[c]	2.295/(2.123)	2.271/(2.171)	2.291/(2.142)	2.269/(2.155)	2.368/(2.337)

[a] Ref. [39].
[b] Ref. [40].
[c] Ref. [41].

Table 2
The optoelectronic parameters of DCJTB films for 12, 22 and 28 μm film thicknesses. (Moss (M), Ravindra (Ra), Hervé-Vandamme (H-V) and Kumar-Singh (K-S)).

Film Thickness (μm)	E_g (eV)	Exp	M	Ra	H-V	K-S
12	2.020	2.892	2.619	2.832	2.672	2.684
22	2.002	2.974	2.625	2.843	2.679	2.692
28	1.996	3.111	2.627	2.847	2.682	2.694

and theoretical method, one can suggest that solution technique gives better results than that of film one.

4.4. Experimental spectral behaviour of transmittance (T)

The transmittance (T) spectra of the solutions of the DCJTB dye for acetone, chloroform, DCM, n-hexane and THF solvents are shown in Fig. 9 (a). From Fig. 9 (a), T spectra of the DCJTB dye for acetone, chloroform, DCM and THF solvents exhibits minimum trenches in the range of 502–509 nm, except n-hexane is 472 nm. After the minimum tendency of the wavelengths of T, a sharply increase is observed up to about 620 nm which is maximum constant value of the wavelengths.

The first derivative $\left(dT/d\lambda\right)$ of T versus λ are plotted to obtain the absorption band edge (E_{g-Abs}) values of DCJTB semiconductor dye for acetone, chloroform, DCM, n-hexane and THF solvents as seen in Fig. 9 (b). E_{g-Abs} values were obtained using the maximum peak position. λ_{max} and E_{g-Abs} for different solvents are tabulated in Table 3. As seen in Table 3, the λ_{max} values of the DCJTB dye for acetone, chloroform, DCM, n-hexane and THF solvents are different. E_{g-Abs} for acetone is found the lowest than that of n-hexane. These results indicate that T spectra of the DCJTB in V region are higher than T spectra in NUV region. Therefore, it is concluded that the solvents have a significant effect on T spectra and absorption band edge of the DCJTB dye.

The α_{mass} values of the DCJTB for acetone, chloroform, DCM, n-hexane and THF solvents were calculated from Eq. (1). Fig. 10 shows α_{mass} plot vs. photon energy (E) of the DCJTB. As seen in Fig. 10, the mass extinction coefficient of the DCJTB dye varies significantly with photon energy. Obtained results indicate that α_{mass} values are the highest for chloroform solvent, while the α_{mass} values are the lowest for n-hexane solvent.

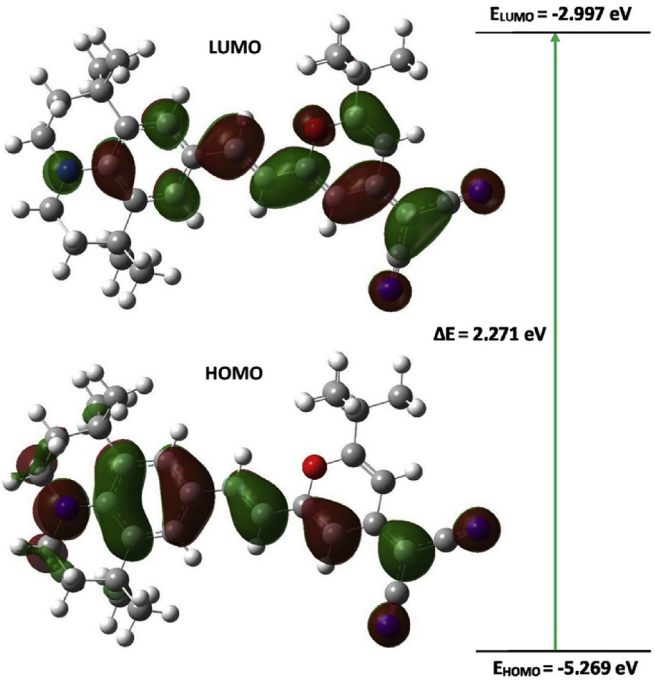

Fig. 8. The molecular orbitals and energy gap (ΔE) between frontier HOMO and LUMO orbitals of DCJTB molecule for Chloroform. Green and red colours represent the positive and negative isosurfaces for HUMO and LUMO, respectively. (For interpretation of the references to colour in this figure legend, the reader is referred to the web version of this article.)

4.5. Experimental optical refractive index

The optical refractive index (n) values of DCJTB films obtained from experimental, Moss, Ravindra, Hervé-Vandamme and Kumar-Singh relations for 12, 22 and 28 μm film thicknesses were given in Table 2. The results show that n of DCJTB films increases with increasing film thicknesses. Fig. 11 indicates n curves depending on film thickness with different relations. From Fig. 11, n values of the DCJTB films increases for all relations with increasing film thicknesses and n values obtained from Moss relation are the lowest, while n values obtained from experiment are the highest. These results show that n of the DCJTB films can be controlled with film thickness and various relations.

n values of the DCJTB dye for acetone, chloroform, DCM, n-hexane and THF solvents with experimental, Moss, Ravindra, Hervé-Vandamme and Kumar-Singh relations were given in Table 3. From Table 3, one can conclude that n can be controlled with solvents. n values of DCJTB dye were obtained for acetone, chloroform, DCM, n-hexane and THF solvents from experimental, Moss, Ravindra, Hervé-Vandamme, and Kumar-Singh relations. The variation of n versus solvents with different relations is shown in Fig. 12. From Fig. 12, n values obtained from Ravindra relation are the highest that of experimental one.

4.6. Theoretical analysis of charge density, Mulliken atomic charge and dipole moment

Charge density picture of DCJTB compound is shown in Fig. 13.

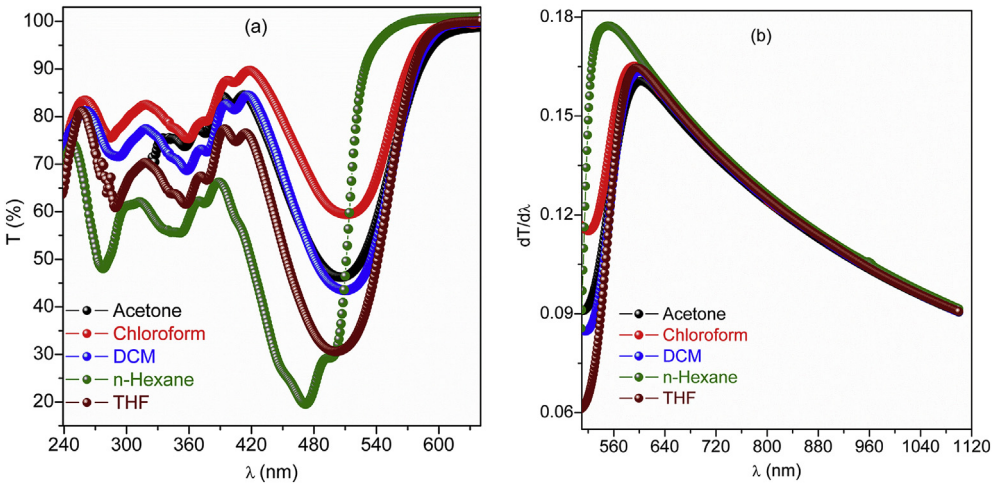

Fig. 9. **(a)** The transmittance (T) and **(b)** $dT/d\lambda$ plots vs. λ of DCJTB solutions for acetone, chloroform, DCM, n-Hexane and THF solvents.

Table 3
The optoelectronic parameters of DCJTB solutions for acetone, chloroform, DCM, n-Hexane and THF solvents. (Moss (M), Ravindra (Ra), Hervé-Vandamme (H-V) and Kumar-Singh (K-S)).

Solvent	λ_{max} (nm)	E_{g-Abs} (eV)	Exp	M	Ra	H-V	K-S
Acetone	602	2.060	2.322	2.586	2.768	2.629	2.641
Chloroform	592	2.095	2.394	2.572	2.738	2.610	2.622
DCM	601	2.063	2.369	2.581	2.756	2.622	2.633
THF	597	2.077	2.468	2.577	2.748	2.616	2.629
n-Hexane	551	2.251	2.315	2.525	2.635	2.547	2.561

As it can be seen from Fig. 13, charge density has a uniform distribution for DCJTB compound considered. The Mulliken atomic charges (MAC) have a significant for quantum mechanical applications. MAC of DCJTB compound were gathered in Table 4. The charges of the atoms in the different positions show different charge with each other for some carbon atoms. For example, MAC of Carbon atom is mostly negative in DCJTB compound, however, the value of the average MAC of this atom is positive in DCJTB compound when carbon atom combined with O and N atoms. The C23 atom exhibits a positive charge the value of MAC is bigger than others. Hydrogen atom exhibits a positive charge because it is an acceptor atom.

The dipole moments are other important electronic properties. The bigger the dipole moment represents the stronger intermolecular interaction. The highest value of component of dipole moment along the x-axis ($\mu_x = -11.77$, Debye) predicts large opposite charge separation in DCJTB compound. The corresponding total dipole moment has been calculated to be 13.27 Debye.

4.7. Theoretical analysis of density of state

The density of states (DOS) is important, because the occupied and unoccupied molecular orbitals can be seen on DOS spectrum. DOS gives a representation of molecule orbitals (MOs) compositions and their contributions to chemical bonding. Using Mulliken population analysis, we have plotted DOS spectrum (see Fig. 14) for DCJTB using GaussSum 3.0 software [42]. From Fig. 14, the density of localized states has a sharply increasing tendency in the region of −10 eV.

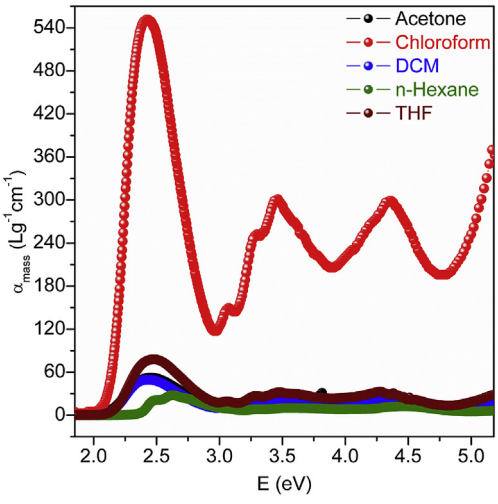

Fig. 10. The mass extinction coefficient (α_{mass}) plot vs. photon energy (E) of DCJTB solutions for acetone, chloroform, DCM, n-Hexane and THF solvents.

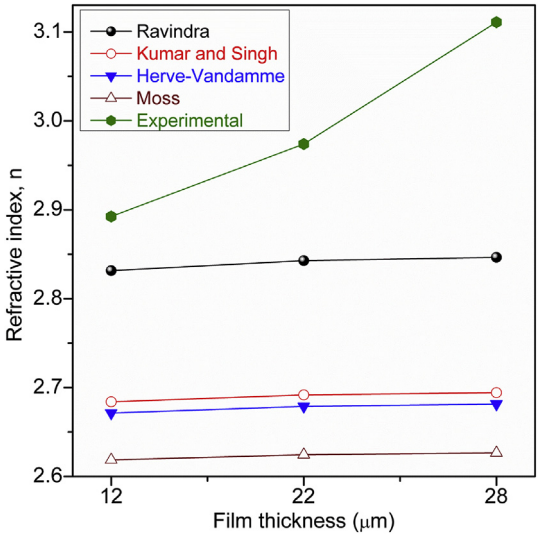

Fig. 11. The refractive index (n) curves of the DCJTB films for 12, 22 and 28 μm obtained from experimental, Moss, Ravindra, Hervé-Vandamme, and Kumar-Singh relations.

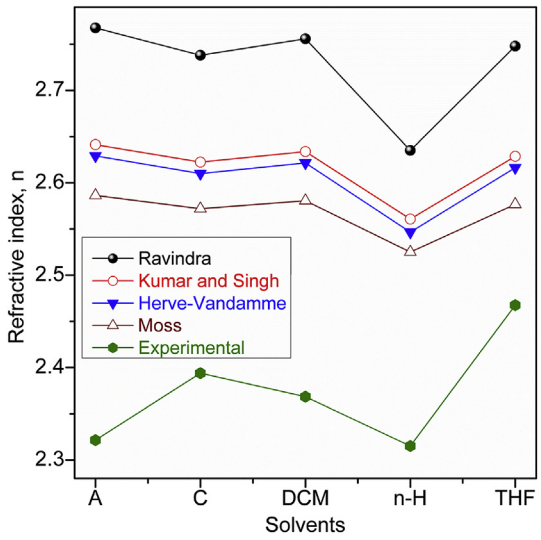

Fig. 12. The optical refractive index (n) curves of the DCJTB solutions for acetone (A), chloroform (C), DCM, n-Hexane (n-H) and THF solvents obtained from experimental, Moss, Ravindra, Hervé-Vandamme, and Kumar-Singh relations.

5. Conclusions

We investigated the structural, electronic and optical properties of DCJTB semiconductor dye by performing both experiments and DFT calculations and analysed in detail. FT-IR analysis indicates that the theoretical scaled wavenumber for acetone solvent is found to be 2960 cm^{-1} which is well matched with experimental value at 2954 cm^{-1}. Theoretically predicted one intense electronic transition for DCJTB with solvent acetone are found as 505.26 nm which is a quite reasonable and agreement with the measured experimental data 505.00 and 503 nm with solution technique and film technique, respectively. The measured HOMO, LUMO and the energy gap values are found to be consistent with the theoretical ones. The obtained energy gap results also indicate that the DCJTB dye exhibits the direct allowed optical band gap, which is desired for optoelectronic devices. Moreover, transmittance spectra of the DCJTB in V region are found to be higher than T spectra in NUV region. The mass extinction coefficient of the DCJTB dye also varies significantly with photon energy. The optical refractive index values of DCJTB films increases with increasing film thicknesses. From the results, one can conclude that the solvents have a significant effect on the optoelectronic properties of DCJTB organic solutions and films and optoelectronic parameters can be controlled with solvents and film thickness. In addition, we presented some results including excess charge on atoms, CD and DOS of the studied molecule using DFT calculations. TD-DFT methods also indicated that solution technique with acetone gives better results than that of thin film. In contrast to film technique, solution is simple, cost-efficient and safe for optoelectronic applications [43]. We hope that this study will provide an insight for new OLED display applications.

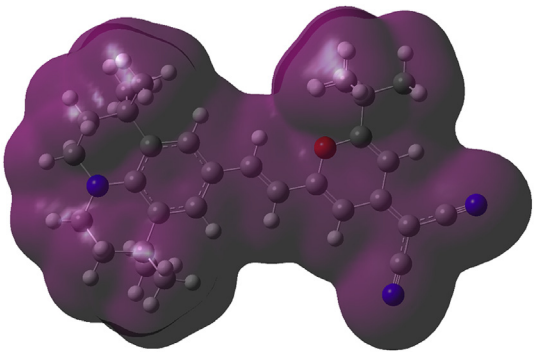

Fig. 13. Charge density picture of DCJTB.

Table 4
Mullkien atomic charges of DCJTB.

Atoms	Mulliken atomic charges	Atoms	Mulliken atomic charges
O1	−0.333499	H36	0.113812
N2	−0.519835	H37	0.114812
N3	−0.241247	H38	0.121138
N4	−0.240861	H39	0.115085
C5	−0.274735	H40	0.108263
C6	−0.278864	H41	0.115008
C7	−0.355411	H42	0.108557
C8	−0.061182	H43	0.108214
C9	−0.069232	H44	0.103702
C10	−0.183977	H45	0.102481
C11	−0.184039	H46	0.114264
C12	−0.022303	H47	0.103167
C13	−0.022114	H48	0.105341
C14	−0.197671	H49	0.103020
C15	−0.231542	H50	0.110541
C16	−0.197284	H51	0.104554
C17	−0.230799	H52	0.114427
C18	−0.016581	H53	0.106677
C19	0.006488	H54	0.104153
C20	−0.087034	H55	0.073118
C21	−0.026245	H56	0.085445
C22	−0.192259	H57	0.117498
C23	0.231847	H58	0.105419
C24	−0.263729	H59	0.124186
C25	−0.240628	H60	0.111417
C26	−0.095789	H61	0.122131
C27	−0.268696	H62	0.115597
C28	−0.240880	H63	0.111383
C29	−0.240639	H64	0.122281
C30	−0.119467	H65	0.124455
C31	0.025751	H66	0.124443
C32	0.062592	H67	0.116022
C33	0.006168	H68	0.115424
C34	0.007108	H69	0.137328
H35	0.121146		

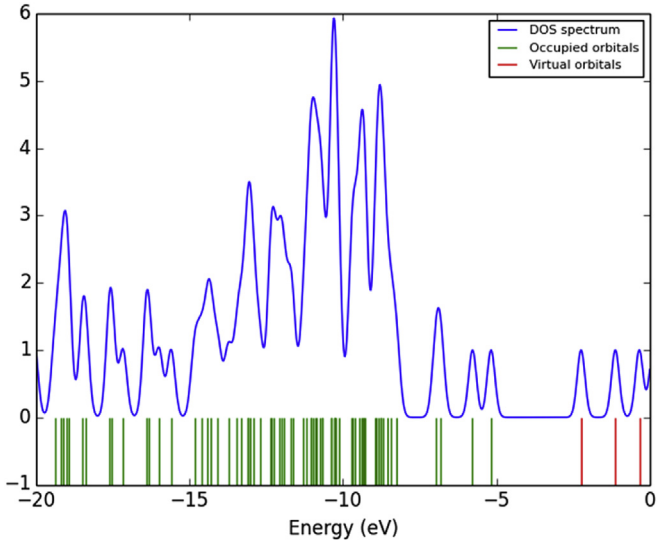

Fig. 14. Density of state (DOS) spectrum of DCJTB obtained Mulliken population analysis.

Acknowledgments

The numerical calculations reported in this paper were partially performed at TUBITAK ULAKBIM, High Performance and Grid Computing Centre (TRUBA resources). The experimental parts of this study were supported by "The Management Unit of Scientific Research Projects of Muş Alparslan University (MUSBAP) under Project MŞÜ14-EMF-G03.

References

[1] T.-Y. Wu, M.-H. Tsao, F.-L. Chen, S.-G. Su, C.-W. Chang, H.-P. Wang, Y.-C. Lin, W.-C. Ou-Yang, I.-W. Sun, Synthesis and characterization of organic dyes containing various donors and acceptors, Int. J. Mol. Sci. 11 (2010) 329–353.
[2] W. Zhou, M.-C. Wang, X. Zhao, Poly(methyl methacrylate) (PMMA) doped with DCJTB for luminescent solar concentrator applications, Sol. Energy 115 (2015) 569–576.
[3] C.-B. Moon, W. Song, M. Meng, N.H. Kim, J.-A. Yoon, W.Y. Kim, R. Wood, P. Mascher, Luminescence of Rubrene and DCJTB molecules in organic light-emitting devices, J. Lumin 146 (2014) 314–320.
[4] D. Xu, Z. Deng, X. Li, Z. Chen, Z. Lv, Non-doped red to yellow organic light-emitting diodes with an ultrathin 4-(dicyanomethylene)-2-tert-butyl-6-(1,1,7,7- tetramethyljulolidin -4-yl-vinyl)-4*H*-pyran (DCJTB) layer, Phys. E 40 (2008) 2999–3003.
[5] R. Gao, Y.X. Cui, X.J. Liu, L.D. Wang, Multifunctional interface modification of energy relay dye in quasi-solid dye-sensitized solar cells, Sci. Rep. 4 (2014), 5570–1-5570-6.
[6] T.-Hsin. Liu, C.-Yeh Iou, C.H. Chen, Doped red organic electroluminescent devices based on a cohost emitter system, Appl. Phys. Lett. 83 (2003) 5241–5243.
[7] Y. Zang, J.-S. Yu, N.-N. Wang, Y.-D. Jiang, Detailed analysis of ultrathin fluorescent red dye interlayer for organic photovoltaic cells, Chin. Phys. B 20 (2011), 017202-1-017202-5.
[8] S.L. Lai, M.F. Lo, M.Y. Chan, C.S. Lee, S.T. Lee, Impact of dye interlayer on the performance of organic photovoltaic devices, Appl. Phys. Lett. 95 (2009), 153303–1-153303-3.
[9] D. Yang, W. Li, B. Chu, Z. Su, J. Wang, G. Zhang, F. Zhang, Enhancement of photovoltaic efficiency of phosphor doped organic solar cell by energy and electron transfer from the phosphor to C60 acceptor, Appl. Phys. Lett. 99 (2011), 193301–1-193301-3.
[10] E.L. Lim, C.C. Yap, M. Yahaya, M.M. Salleh, M.H.H. Jumali, ZnO nanorod arrays pre-coated with DCJTB dye for inverted type hybrid solar cells incorporating P3HT donor, J. Mater Sci. Mater Electron 26 (2015) 719–725.
[11] D. Zhang, Z. Duan, Y. Wang, P. Zhang, S. Chen, Amplified spontaneous emission from DCJTB encapsulated in mesostructured composite silica SBA-15, Appl. Opt. 55 (2016) 4736–4740.
[12] B. Gündüz, Investigation of the spectral, optical and surface morphology properties of the N,N′-Dipentyl-3,4,9,10-perylenedicarboximide small molecule for optoelectronic applications, Polym. Adv. Technol. 27 (2016) 144–155.
[13] B. Gündüz, Optical properties of poly[2-methoxy-5-(3′,7′-dimethyloctyloxy)-1,4-phenylenevinylene] light-emitting polymer solutions: effects of molarities and solvents, Polym. Bull. 72 (12) (2015) 3241–3267.
[14] J. Tauc, Amorphous and Liquid Semiconductors, Plenum Press, New York, 1974.
[15] A. Kurt, Influence of $AlCl_3$ on the optical properties of new synthesized 3-armed poly(methyl methacrylate) films, Turk. J. Chem. 34 (2010) 67–79.
[16] N. Turan, E. Kaya, B. Gündüz, N. Çolak, H. Körkoca, Synthesis, characterization of poly(E)-3-amino-4-((3-bromophenyl)diazenyl)-1H-pyrazol-5-ol: investigation of antibacterial activity, fluorescence, and optical properties, Fiber. Polym. 13 (4) (2012) 415–424.
[17] S.K. Tripathy, Refractive indices of semiconductors from energy gaps, Opt. Mater 46 (2015) 240–246.
[18] N.M. Ravindra, S. Auluck, V.K. Srivastava, On the penn Gap in semiconductors, Phys. Status Solidi B 93 (1979) K155–K160.
[19] P. Hervé, L.K.J. Vandamme, General relation between refractive index and energy gap in semiconductors, Infrared Phys. 35 (1994) 609–615.
[20] W. Kohn, L.J. Sham, Self-consistent equations including exchange and correlation effects, Phys. Rev. 140 (1965) A1133–A1138.
[21] A.D. Becke, Density-functional exchange-energy approximation with correct asymptotic behavior, Phys. Rev. A 38 (1988) 3098–3100.
[22] S.H. Vosko, L. Vilk, M. Nusair, Accurate spin-dependent electron liquid correlation energies for local spin density calculations: a critical analysis, Can. J. Phys. 58 (1980) 1200–1211.
[23] C. Lee, W. Yang, R.G. Parr, Development of the Colle-Salvetti correlation-energy formula into a functional of the electron density, Phys. Rev. B 37 (1988) 785–789.
[24] M.J. Frisch, G.W. Trucks, H.B. Schlegel, G.E. Scuseria, M.A. Robb, J.R. Cheeseman, G. Scalmani, V. Barone, B. Mennucci, G.A. Petersson, et al., Gaussian 09, Revision B.01, Gaussian, Inc., Wallingford CT, 2009.
[25] A. Janani, R.S. Skylab, Injectable hydrogel for cardiac tissue engineering, IJCRGG 6 (2014) 2233–2236.
[26] J. Sylvia, J. Lakshmi, R. Devi, Purification and characterization of manganese peroxidase from musa acuminata stem and its effect on degradation of dye effluent, Int. J. Innov. Res. Sci. IJIRSET 4 (2015) 2981–2987.
[27] V.Z. Guorong, H. Yang Jr., Ross N. Philip, K. Xu, J.T. Richard, Lithium methyl carbonate as a reaction product of metallic lithium and dimethyl carbonate, Lawrence Berkeley National Laboratory, http://escholarship.org/uc/item/93b8h284, 2005. Accessed 12 July 2016.
[28] G. Madhurambal, B. Ravindran, M. Mariappan, Thermal, UV and FTIR spectroscopic studies of mercury cinnamate, Asian Journal of Chemistry, Asian J. Chem. 23 (2011) 917–918.
[29] B. Nandapure, S. Kondawar, M. Salunkhe, A. Nandapure, Nanostructure cobalt oxide reinforced conductive and magnetic polyaniline nanocomposites, J. Compos. Mater 47 (5) (2013) 559–567.
[30] R.K. Saini, D. Singh, S. Bhagwan, S. Verma, Sonika, P.S. Kadyan, Characterization of near infrared light emitting (benzene-co-pentacene) copolymer, Der Pharma Chem. 6 (4) (2014) 255–260.
[31] A. Rahimpour, S.S. Madaeni, S. Zereshki, Y. Mansourpanah, Preparation and characterization of modified nano-porous PVDF membrane with high anti-fouling property using UV photo- grafting, Appl. Surf. Sci. 255 (2009) 7455–7461.
[32] B.J. Saikia, G. Parthasarathy, Fourier transform infrared spectroscopic characterization of kaolinite from Assam and Meghalaya, N. India, J. Mod. Phys. 1 (2010) 206–210.
[33] Ashish Patel, T.Y. Pasha, Reena Kothari, Synthesis and biological evaluation of some novel heterocyclic compounds as protein tyrosine phosphatase (PTP-1B) Inhibitor, J. Chem. Pharm. Res. 7 (10) (2015) 509–517.
[34] S. Zuo-Sen, Z. Xiao-Long, W. Shi-Wei, Z. Li-Sha, C. Zhan-Chen, Synthesis and non-linear optical (NLO) properties of a series of alkoxysilane derivative chromophores, Chem. Res. Chin. Univ. 25 (5) (2009) 775–780.
[35] Bhaskar J. Saikia, G. Parthasarathy, N.C. Sarmah, Fourier transform infrared spectroscopic characterization of dergaon H5 chondrite: evidence of aliphatic organic compound, Nat. Sci. 7 (5) (2009) 45–51.
[36] Abha Misra, Pawan K. Tyagi, M.K. Singh, D.S. Misra, FTIR studies of nitrogen doped carbon nanotubes, Diam. Relat. Mater 15 (2–3) (2006) 385–388.
[37] J.V. Gulmine, P.R. Janissek, H.M. Heise, L. Akcelrud, Polyethylene characterization by FTIR, Polym. Test. 21 (2002) 557–563.
[38] M. Kurban, Ş. Erkoç, Structural and electronic properties of $Zn_mCd_nTe_k$ (m+n+k=2-4) clusters: DFT calculations, J. Comput. Theor. Nanosci. 12 (2015) 2605–2615.
[39] M-Ying Chang, Y-Kai Han, C-Chih Wu, S-Chin Lin, W-Yao Huang, High-efficiency red organic light emitting diodes incorporating 1,3,5-tris(1-pyrenyl) benzene as the host material, J. Electrochem. Soc. 155 (12) (2008) J345–J349.
[40] K.H. Lee, S.H. Oh, M.H. Park, Y.K. Kim, S.S. Yoon, An efficient red organic light-emitting diode using DCJTB type emitters based on silicone containing julolidine derivatives, Mol. Cryst. Liq. Cryst. 550 (2011) 270–277.
[41] D. Xu, X. Li, H. Ju, Y. Zhu, Z. Deng, A novel red organic light-emitting diode with ultrathin DCJTB and Rubrene Layers, Displays 32 (2011) 92–95.
[42] N.M. O'Boyle, A.L. Tenderholt, K.M. Langer, A library for package-independant computational chemistry algorithms, J. Comput. Chem. 29 (2008) 839–845.
[43] B. Gündüz, Effects of molarity and solvents on the optical properties of the solutions of tris[4-(5-dicyanomethylidenemethyl-2-thienyl)phenyl]amine (TDCV-TPA) and structural properties of its film, Opt. Mater 36 (2) (2013) 425–436.